HHS Public Access

Author manuscript

Genet Med. Author manuscript; available in PMC 2021 November 28.

Published in final edited form as:

Genet Med. 2021 October ; 23(10): 1864–1872. doi:10.1038/s41436-021-01224-8.

X-linked Creatine transporter deficiency results in prolonged QTc and increased sudden death risk in humans and disease model

Mark D. Levin[1,*,†], **Simona Bianconi**[2,*], **Andrew Smith**[2], **Niamh X. Cawley**[2], **An Dang Do**[2], **Dylan Hammond**[2], **Julia F. Grafstein**[2], **Audrey Thurm**[3], **Judith Miller**[4,5], **John Perreault**[2], **Audrey Noguchi**[6], **Danielle Springer**[6], **Beth A. Kozel**[1], **Christopher F. Spurney**[7], **Christopher A. Wassif**[2], **Zu-Xi Yu**[8], **Andreas Schulze**[9], **Forbes D. Porter**[2], **Fady Hannah-Shmouni**[2]

[1.]Translational Vascular Medicine Branch, National Heart, Lung and Blood Institution, National Institutes of Health (NIH) Bethesda, Maryland, USA

[2.]Division of Translational Medicine, *Eunice Kennedy Shriver* National Institute of Child Health and Human Development, National Institutes of Health (NIH), Bethesda, Maryland, USA

[3.]National Institute of Mental Health, National Institutes of Health (NIH), Bethesda, Maryland, USA

[4.]Center for Autism Research, Children's Hospital of Philadelphia, Perelman School of Medicine, University of Pennsylvania, Philadelphia, PA, USA

[5.]Division of Developmental and Behavioral Pediatrics, Children's Hospital of Philadelphia, Perelman School of Medicine, University of Pennsylvania, Philadelphia, Pennsylvania, USA

[6.]Murine Phenotyping Core, National Heart, Lung and Blood Institution, National Institutes of Health (NIH) Bethesda, Maryland, USA

[†]**Corresponding author:** Mark D. Levin, M.D., Translational Vascular Medicine Branch, National Heart, Lung, Blood Institutes, NIH, Bethesda, MD 20892, Mark.Levin@nih.gov, Cell phone: (215) 485-3900.

[*]Authors contributed equally

Author Contributions

Conceptualization: MDL, SB, FDP; Data curation: MDL, SB, ASM. NXC, ADD, DH, JFG, AT, JM, JP, NG, DS, CFS, CAW, ZXY, ASC, FDP, FHS; Formal analysis: MDL, SB, ASM. NXC, ADD, JFG, AT, JM, NG, DS, BK, CFS, CAW, ZXY, ASC, FDP, FHS; Funding acquisition: FDP Investigation: MDL, SB, ASM. NXC, ADD, JFG, NG, DS, ZXY,CAW, FDP, FHS; Methodology: MDL, SB, ADD, FDP, ZXY, FHS; Supervision: MDL, SB, FDP, FHS Visualization: MDL, ZXY, ASM, FHS; Writing & editing: MDL, SB, ASM, NXC, ADD, DH, JFG, AT, JM, JP, NG, DS, CFS, CAW, ZXY, BK, ASC, FDP, FHS;

Conflict of interest declaration: The authors declare no conflict of interest

Trial Registration: ClinicalTrials.gov Identifier: NCT02931682

Data availability: Data will be made available upon request to first, corresponding or senior authors. Genomic data will be made available provided related NIH and NICHD privacy guidelines can be fully met. Deidentified genomic data will be provided upon request.

Ethics Declaration:

a. Study approval was obtained from the IRB at the National Institute of Child Health and Human Development (NICHD), NIH. All guidelines for good clinical practice were followed. Guardians provided written consent. Assent was obtained when possible.

b. Animal studies: All studied experiments performed had prior approval from NICHD animal studies committee and were carried out in strict compliance with all NIH guidelines and ethical regulations.

Ethics statements

1. This study was reviewed by the NICHD IRB and was approved prior to all research.
2. We have explicitly obtained written consent for every patient whose data has been included in this study.
3. Each author has reviewed the manuscript and has agreed to its submission.

[7]Division of Cardiology, Department of Pediatrics, Children's National Medical Center Washington, DC, USA

[8]Pathology Core, National Heart, Lung and Blood Institution, National Institutes of Health (NIH) Bethesda, Maryland, USA

[9]Departments of Pediatrics and Biochemistry, Research Institute, Hospital for Sick Children, University of Toronto, Toronto, Canada

Abstract

Purpose: Creatine transporter deficiency (CTD) is a rare X-linked disorder of creatine transport caused by pathogenic variants in *SLC6A8* (Xq28). CTD features include developmental delay, seizures and autism spectrum disorder. This study was designed to investigate CTD cardiac phenotype and sudden death risk.

Methods: We performed a cross-sectional analysis of CTD males between 2017–2020. Subjects underwent evaluation with ECG, echocardiography and ambulatory ECG with comparable analysis in creatine transporter deficient mice (*Slc6a8*$^{-/y}$) using ECG, echocardiography, exercise testing and indirect calorimetry.

Results: Eighteen subjects with CTD [18 males, age 7.4 (3.8) years] were evaluated: seven subjects (39%) had QTc≥470msec: 510.3±29.0 vs. 448.3±15.9, P<0.0001. The QTc≥470msec cohort had increased left ventricular internal dimension(diastole) ((LVIDd) Z-score: 0.22±0.74, n=7 vs. −0.93±1.0, n=11, P=0.0059), and diminished left ventricular posterior wall dimension(diastole)((LVPWDd, in mm): 5.0±0.6, n=7 vs. 5.7±0.8, n=11, P=0.0183), when compared to subjects with normal or borderline QTc prolongation. Similar ECG and echocardiographic abnormalities were seen in *Slc6a8*$^{-/y}$ mice. Additionally, *Slc6a8*$^{-/y}$ mice had diminished survival (65%).

Conclusions: Prolonged QTc and abnormal echocardiographic parameters consistent with developing cardiomyopathy are seen in some male subjects with CTD. *Slc6a8*$^{-/y}$ mice recapitulated these cardiac abnormalities. Male CTD subjects may be at increased risk for cardiac dysfunction and sudden death.

INTRODUCTION

Creatine transporter deficiency (OMIM 300352; CTD) is a rare X-linked disorder of creatine transport caused by pathogenic variants in the creatine transporter protein encoded by *SLC6A8* mapping to Xq28[1,2]. CTD is estimated to affect 0.3%−3.5% of males with intellectual disability[3,4]. Creatine functions as both a source and a sink of high energy phosphate bonds, facilitating the transport of high energy bonds across membranes. Creatine is synthesized predominantly in the liver, so its presence in the brain, heart and skeletal muscle requires active transport using SLC6A8[5]. Strong expression of this protein has been confirmed in human hearts[6,7]. A deficiency of this system, first described in 2001,[8] manifests with developmental delay, hypotonia, autism spectrum disorder, failure to thrive, and seizures[9].

The literature contains little about CTD cardiac manifestations, despite the heart's high energy demands. A retrospective study of 101 CTD males showed (ages 1–66 years, median 10 years) two subjects had mild cardiomyopathy, 1 subject had premature ventricular contractions(PVC's), and one subject had a prolonged QTc (nearly 500msec)[9]. A separate case report detailed the course of a CTD subject who had frequent PVC's[10].

While SLC6A8 is highly expressed in skeletal and cardiac muscles, observable cardiomyopathy is not a consistently reported feature of CTD. Germline creatine transporter knockout mice (*Slc6a8*$^{-/y}$), showed reduced, but not absent, creatine levels. Those caring for CTD subjects suspect sudden death occurs among patients. Review of the literature revealed one CTD case of a child who died suddenly at 17yo[11].

Prolonged QTc defines a handful of monogenic disorders that comprise Long QT Syndrome (LQTS) which causes ventricular fibrillation and sudden death. A QTc interval is considered prolonged if it exceeds 450msec. However, this mortality risk increases significantly when the QTc exceeds 500msec[12].

The purpose of this study was to characterize cardiovascular disease arising from CTD and investigate its mechanistic basis using animal models. Prior studies using this X-linked model of creatine transporter deficiency (*Slc68a*$^{-/y}$)[13,14] confirmed reduced brain (and heart) creatine levels matching human disease levels and corroborated the presence of behavioral and cognitive deficits in the model that recapitulate human CTD cognitive abnormalities including impaired object recognition as well as spatial and memory function deficits. We hypothesized that QTc prolongation occurs with increased frequency in CTD patients and speculate this may contribute to increased sudden death risk in CTD patients. Our *Slc68a*$^{-/y}$ studies demonstrate reduced model body weight similarly described in initial studies[13] that match subject BMI abnormalities (Supplemental Table 1). Further, our studies demonstrate that the *Slc68a*$^{-/y}$ model recapitulates critical aspects of CTD cardiac disease by displaying abnormal cardiac repolarization, cardiomyopathy-like features, and decreased survival suggestive of increased sudden death risk, marking this model as an essential tool for elucidating human CTD disease mechanisms and potential therapeutics.

MATERIALS AND METHODS

Human subjects

Study approval was obtained from the IRB at the National Institute of Child Health and Human Development (NICHD), NIH. All guidelines for good clinical practice were followed. Guardians provided written consent. Assent was obtained when possible. Data for all subjects were obtained under a protocol titled 'Observational Study of Males with Creatine Transporter Deficiency (Vigilan), NCT02931682. CTD diagnosis was confirmed by ascertaining a pathogenic variant in *SLC6A8* through direct exome sequencing (Supplemental Table 2), as well as biochemical confirmation of elevated creatine to creatinine ratio in urine. Standard clinical histories and physical examination were obtained. Medications were reviewed [15,16]. Genetic testing for genes associated with LQTS was performed by a CLIA-certified laboratory, GeneDx (Supplementary Table 3).

Human ECG examination

Standard ECG equipment was used to record 12-lead ECGs. All ECGs were reviewed by a pediatric cardiologist (MDL) and QTc intervals were manually calculated using Bazett equation[17]. For subjects who had more than one ECG, the longest QTc for each subject was used. A QTc cutoff of ≥470msec was chosen to define prolongation, as it represents the 99th percentile for QTc length[17].

Human echocardiographic examination

Complete transthoracic echocardiograms using M-mode, 2-dimensional (2D) and color Doppler were performed in all study participants using commercially available systems[18].

Human ambulatory ECG examination

Standard commercially available three lead ambulatory ECG monitors were used to perform 24-hour monitoring on subjects and all data were reviewed by telemetry nurse and a pediatric cardiologist (MDL). Studies were considered complete when there was >22hours of recordings that had less than 5% artifact during the recording time. Eleven of eighteen subjects were able to complete these recordings.

Creatine transporter knockout mice (*Slc6a8*$^{-/y}$)

All mouse studies were performed according to NIH guidelines and approved by the NICHD Animal Care and Use Committee. Generation of the *Slc68a*$^{-/y}$ has been previously described[13] and mice were graciously provided by those authors. Mice were housed at ~22 ° C with a 12:12-h light-dark cycle. Chow (NIH-07, Envigo Inc, Madison, WI) and water were available ad libitum. NIH-7 rodent chow contains small but undefined amounts of creatine due to fish meal ingredients (approximately 0.001% creatine, Dr. Schulze, own observation).

Mouse ECG readings

Multi-lead ECGs were collected from isoflurane anesthetized mice at roughly 8 weeks of age using PowerLab (ADInstruments)[19]. Two blinded researchers (JFG and MDL) calculated three separate measurements for the following: PR, QRS, RR and QT intervals from each mouse. The end of the slow T-wave component was estimated by extending a baseline from the isoelectric portion of the PR interval and determining where T-wave crossed this baseline. Corrected QT (QTc) intervals were calculated using standard Bazett formula. Cohort mean±SD were tested for significance using the Mann-Whitney.

Mouse echocardiographic examination

Mice were anesthetized with 1.75% isoflurane and were placed on a heated platform equipped with ECG and respiratory rate monitors. Echocardiography was performed with a high-frequency linear array ultrasound system (Vevo 2100, VisualSonics) and MS-400 30 MHz transducer (VisualSonics). Complete 2D transthoracic images were obtained. Fractional shortening(FS) and ejection fraction(EF) were calculated from parasternal short axis in M-mode. For 3-month echocardiographic evaluation, 5 male *Slc68a*$^{-/y}$ mice were studied initially, along with 5 gender-matched littermate controls. Subsequent analysis revealed one control mouse demonstrated valvar pulmonary stenosis with thickened valve

leaflets and doppler flow acceleration consistent with mean gradient between 20–30mmHg; this control data was excluded.

Mouse body composition measurements

Whole-body composition was obtained as described previously[20] using nuclear magnetic resonance. The EchoMRI (EchoMRI LLC, Houston, TX) was used to scan unanesthetized mice to estimate the mass of lean and fat tissue.

Mouse indirect calorimetry

Open circuit calorimetry, activity, and food consumption data were collected using the Oxymax Comprehensive Laboratory Animal Monitoring System (CLAMS, Columbus Instruments, Columbus, OH). Mice (n=5 per group per age) were housed individually in the calorimetry cages for 5 days while metabolic parameters were measured. Twelve-hour light–dark phase cycles and standard animal room temperature (24^{o}C) were maintained and water and food were provided ad libitum and carefully quantified. Oxygen consumption (VO_2) was normalized to body weight (BW)^0.75[21].

Mouse exercise stress testing (EST)

Exercise capacity was tested using a Columbus Instruments rodent treadmill (Model Eco-6M), set at a 10 degree incline[22]. Testing protocol: 10 min with belt speed at 10 m/min, 12 m/min for five minutes, 15 m/min for three minutes and then the belt speed was increased incrementally by 1.8 m/min every three minutes until the mouse became exhausted. Total time, distance, maximum speed, and work were recorded at the time of exhaustion, defined as when mice were unable to continue running without repeatedly falling back onto the shock grid at the back of treadmill.

Histology

Hearts were harvested from 9month old mice, aorta's were cannulated and 4% paraformaldehyde was retrogradely perfused and allowed to dwell for 48hours. Hearts were then dehydrated in 50%, 75%, 95% and 100% alcohols over 5 days. Tissue was embedded in paraffin, and cut to 5um thick sessions for subsequent staining using standard H&E or Masson's trichrome methods.

Statistical Analysis

Data is displayed as mean±SD unless otherwise noted. Mann-Whitney tests were used to test for significance unless noted otherwise. Statistics were performed using GraphPad Prism version 8.0.0 for Mac, GraphPad Software, San Diego, California USA, www.graphpad.com, except simple linear regression analysis was performed using the "lm" function in R[23] and plotted using ggplot2[24].

RESULTS

Human Clinical and Genetic data

We performed a cross-sectional analysis of clinical, biochemical, and radiological characteristics of 18 males with CTD [age 7.4±3.8 years, Supplemental Table 1] at the NIH. Supplemental Table 4 lists all medications for each subject. No medication or supplement has been reported to prolong QTc (qtdrugs.org). Several subjects had prior seizure disorder diagnoses. LQTS can masquerade as seizure disorder. However, no subject in our cohort had a family history consistent with LQTS. To explore the possibility that QTc prolongation resulted from metabolic acidosis, we performed linear regression and found no correlation between QTc length and serum acidosis (Supplemental Figure1).

To determine if any member of our cohort harbored a pathogenic variant in a known LQTS gene, genomic DNA was sent to test for channelopathy (GeneDx, Supplemental Table 3). While we were unable to obtain gene panel evaluations in 2 subjects in the “normal/borderline” prolonged QTc cohort, no QT prolonging variant was detected by genetic testing in the remaining cohort.

Human ECG

ECG parameters were evaluated on 18 subjects (Table 1). Eleven subjects had QTc intervals <470msec (borderline QTc cohort), while seven subjects had prolonged QTc>470 (prolonged QTc cohort). Figure 1 demonstrates an ECG from a subject with “normal” QT interval (Fig 1A), and one with a prolonged QTc (Fig. 1B). In panel 1B, the displayed T-wave not only shows a prolonged QT interval, but also demonstrates abnormal T-wave morphology (Figure 1C, lead III). By comparison, Figure 1C lead V6 demonstrates a normal QRS:T-wave relationship. Lead aVF in Figure 1C shows “T-wave flattening.” Both T-wave inversion and T-wave flattening are abnormal, and their presence should prompt a cardiomyopathy evaluation. Figure 1D shows a scatter plot demonstrating the QTc distribution for each cohort. Three of 11 subjects with QTc <470msec, and 6 of 7 subjects with QTc ≥470msec demonstrated inferior lead T-wave abnormalities.

Human Echocardiography

Echocardiograms were obtained in 18 subjects (Table 1). No subject demonstrated congenital heart malformation. All subjects demonstrated normal systolic function. Interestingly, subjects with a longer QTc intervals had increased LV internal dimension(diastole)((LVIDd) z-score, (QTc<470msec: −0.93±1.0, n=11; vs. QTc≥470msec: 0.22±0.74, n=7, $P=0.0059$). Furthermore, subjects with longer QTc intervals also were more likely to show left ventricular posterior wall dimension(diastole)((LVPWDd) thinning (in mm): QTc<470msec: 5.7±0.8, *n=11 vs* QTc≥470msec: 5.0±0.6, n=7, P=0.0183). Figure 1 demonstrates LVIDd z-score (panel E), LVPWDd z-score (panel F) and LV mass index z-score (panel G). While normal systolic function precludes cardiomyopathy diagnosis, dilating chamber and wall thinning suggest possible developing cardiomyopathy.

Human ambulatory ECG

Eleven subjects tolerated ambulatory ECG monitors (Supplemental Table 5). No subject demonstrated rhythm abnormality.

Our initial investigations suggested CTD subjects displayed abnormal ECG's and echocardiograms consistent with developing cardiomyopathy. Given that sudden death is rare and our cohort is small, we obtained a mouse model of creatine transporter knockout (*Slc6a8*$^{-/y}$) to further investigate the biologic consequences of *Slc6a8* disruption[13,14].

Mouse Electrocardiogram

We sought to confirm whether *Slc6a8*$^{-/y}$ mice expressed prolonged QTc intervals. Figure 1 demonstrates representative ECG traces (control, *Slc6a8*$^{+/y}$, Fig. 1H*; Slc6a8*$^{-/y}$ mice, Fig. 1I). Figure 1 demonstrates the T-wave start (T_0) at the completion of the QRS complex and its termination (T_f). Two researchers, blinded to genotype, quantified PR, QRS, RR and QTc interval durations (Figure 1H-L, Supplemental Table 6). Mean QTc(in seconds) was significantly prolonged (*Slc6a8*$^{-/y}$ mean=0.1829±0.0370sec; *Slc6a8*$^{+/y}$ mean= 0.1435±0.02114sec; *P=0.0185*), and *Slc6a8*$^{-/y}$ demonstrated slightly increased QRS interval (QRS: *Slc6a8*$^{+/y}$:12.50±0.27msec vs *Slc6a8*$^{-/y}$: 14.50±0.43msec; *P=0.0022*).

Mouse Echocardiogram

Slc6a8$^{-/y}$ mice showed echocardiographic abnormalities similar to those seen in CTD subjects. Echocardiograms were first performed at 3 months. Figure 2C-H summarizes those findings. *Slc6a8*$^{-/y}$ mice showed normal systolic function (Fig. 2C., Fractional shortening, (FS) (in %): control: 34.68% vs *Slc6a8*$^{-/y}$: 37.72%; (normal >28%)). As in CTD subjects, *Slc6a8*$^{-/y}$ displayed significant chamber dilation at 3 months of age (Fig. 2E, LVIDd(indexed)(in mm/g): *Slc6a8*$^{+/y}$:0.1459±0.0093 vs *Slc6a8*$^{-/y}$: 0.1936±0.0063; *P=0.000036)*. While CTD human subject LV chamber wall appeared thinned compare to controls, *Slc6a8*$^{-/y}$ mice displayed *increased* LV chamber wall thickness (Fig. 2G, LVPWDd, indexed (in mm/g)), (LVPWDd: *Slc6a8*$^{+/y}$: 0.02885±0.009 *Slc6a8*$^{-/y}$: 04508±0.00096, *P<0.000001*).

Repeat echocardiographic assessment in the identical mice was performed at 9 months to assess for potential age-related effects. Figure 2 allows for parameter comparison at both 3 and 9 months. While we saw no statistically significant differences in chamber dimensions between 3 and 9 months, one can see a precipitous drop in systolic function in one *Slc6a8*$^{-/y}$ mouse (Fig2C, 9mo). Notably, two *Slc6a8*$^{-/y}$ mice died unexpectedly within a week of these studies, including one mouse with the lowest FS of the cohort (FS=33%; EF=63% (normal)). Cardiac tissue from the remaining mice was harvested and analyzed using H&E and Masson's trichrome, but no differences in cellular morphology or fibrosis were found (Supplmental Figure 2).

Mouse Indirect Calorimetry (CLAMS)

As both our subject and animal model echocardiography studies demonstrated evidence of possible cardiomyopathy, and the defect central to CTD involves energy/metabolite transfer, we sought to quantify food intake, activity, and oxygen consumption as a means of further

delineating the model disease course. Others have proposed that cardiomyopathy arising from mutated sarcomeric proteins is correlated with inefficient energy use which ultimately results in energy depletion[25,26]. Thus, determining the model's energy usage seemed an appropriate next step in elucidating cardiac disease mechanisms. Figure 3 summarizes normalized food intake (Fig. 3A), total activity (Fig. 3B) and normalized total oxygen consumption (Fig. 3C). Figure 3 also displays body composition parameters including weight(grams) (Fig. 3D), Fat mass (Fig. 3E), %Fat mass (Fig. 3F), Lean mass (Fig. 3G), and %Lean mass (Fig. 3H). *Slc6a8*$^{-/y}$ mice demonstrate diminished weight, fat mass, and lean mass (%lean mass possibly trending significant P=0.0952). While activity is roughly equivalent between *Slc6a8*$^{-/y}$ mice and controls (Fig. 3B), oxygen consumption (VO_2) is significantly increased in *Slc6a8*$^{-/y}$ mice. Additional analyses demonstrated a *Slc6a8*$^{+/y}$ mean $V0_2$=3163±420 ml/kg/hr, while for *Slc6a8*$^{-/y}$ mean=4290±597 ml/kg/hr (P<0.0001, Mann-Whitney). Consistent with this increase in $V0_2$, there is increased food intake, presumably to maintain adequate energy stores. Thus, the 3-month indirect calorimetry data suggested *Slc6a8*$^{-/y}$ energy metabolism was significantly less efficient than control. As with echocardiography studies, we repeated indirect calorimetry at 9 months, but saw no significant differences in findings when compared to those performed at 3 months (Supplemental Figure 3).

Mouse Exercise Stress Test

To further characterize *Slc6a8*$^{-/y}$ mouse cardiovascular function, we exercised 3-month-old mice using motorized treadmill apparatus in a run-to-exhaustion format (Fig. 3I-K). Using identical protocols, *Slc6a8*$^{-/y}$ mice showed significant diminished work capacity (Fig. 3J, Work(in kg/m), *Slc6a8*$^{+/y}$: 3.48±0.52 vs *Slc6a8*$^{-/y}$: 1.052±0.140; *P<0.0001*). Furthermore, *Slc6a8*$^{-/y}$ mice were not able to run as far as controls (Fig. 3I, Distance(meters), *Slc6a8*$^{+/y}$: 745.4±106.4m vs *Slc6a8*$^{-/y}$: 370.8±46.3m; P<0.0001), and they fatigued more quickly than their control counterparts (Fig. 3K, Time to exhaustion (minutes), *Slc6a8*$^{+/y}$: 41.3±3.7 vs *Slc6a8*$^{-/y}$: 26.8±2.1; *P<0.0001*).

Premature death in Slc6a8$^{-/y}$ mice

Strikingly, we found *Slc6a8*$^{-/y}$ mice died earlier than control littermates. Specifically, 12 of 28 *Slc6a8*$^{-/y}$ mice (42.9%) died unexpectedly, while only 1 of 70 *Slc6a8*$^{+/y}$ mice (1.4%) died unexpectedly during the same 40-week time period. Figure 4 shows a Kaplan-Meier-like survival curve (P=0.0005, Log-rank (Mantel-Cox) test).

DISCUSSION

CTD subjects show prolonged QTc and evidence of cardiomyopathy

This prospective study was designed to analyze the cardiac phenotype of CTD patients. Review of ECG and echocardiograms showed a surprisingly large percentage of CTD subjects with QTc prolongation. Seven of eighteen subjects had a QTc > 470msec, representing >99th percentile for QTc length. Of the 11 subjects in the "normal or borderline" prolonged QTc group, seven of those subjects had "borderline" QTc prolongation, with QTc intervals between 450–470msec. Further investigation of all subjects identified no primary channelopathy or medication that otherwise explains QTc

prolongation. Thus, we strongly suspect QTc prolongation arises as a direct consequence of CTD cardiac pathology. Hyperdynamic function seen in *Slc6a8*$^{-/y}$ mice suggests remodeling includes increased inward calcium current. Consistent with these findings, we found that those subjects with "prolonged" QTc, were more likely to have inferior lead T-wave abnormalities (6 of 7 subjects in this cohort), suggesting potassium channel remodeling as well as possible cardiomyopathy development[27].

CTD subject echocardiography findings also suggest possible ion channel remodeling. We found those in the "prolonged" QTc cohort had increased LVIDd and LVIDd z-score, consistent with a more dilated LV chamber, and thinner ventricular chamber wall dimension (LVPWDd). These findings are cardinal features of a dilated cardiomyopathy. While no subject had depressed cardiovascular systolic function, one could argue that chamber dilation and wall thinning suggest a developing cardiomyopathy process.

CTD mouse model recapitulates human QTc prolongation and aspects of cardiomyopathy

As we sought to investigate mechanisms underlying CTD subject cardiac disease, we performed ECG and echocardiography studies in a mouse model. Mirroring abnormalities found in human subjects, *Slc6a8*$^{-/y}$ mouse ECG recordings showed significantly prolonged QTc intervals (Fig. 1H-J). Furthermore, mouse echocardiography also demonstrated increased LV chamber dimension with preserved systolic function (Fig. 2C, E). Unlike human subjects, however, model LV wall thickness showed hypertrophy rather than wall thinning (Fig. 2G), suggesting hypertrophic cardiomyopathy process. Indirect calorimetry and exercise stress test results further suggest a cardiomyopathy picture: indirect calorimetry measurements are consistent with inefficient metabolism in *Slc6a8*$^{-/y}$ mice. We found markedly increased VO_2, diminished exercise work and distance in addition to shorter time to exhaustion in *Slc6a8*$^{-/y}$ mice. A hallmark of cardiomyopathies is that they are often caused by pathogenic variants in sarcomeric genes that result in inefficient energy utilization[25]. The greatly increased VO_2 likely reflects such an inefficiency that remains compensated for in the 3-month old mice. By 9 months however, we see two mice died suddenly. These studies not only support the hypothesis that *Slc6a8* deletion results in cardiomyopathy, more importantly, it may suggest a possible mechanism that contributes to this cardiac phenotype.

Metabolic abnormalities underlie cardiac structural and repolarization abnormalities

Two potential mechanisms could account for how creatine transport deficiency gives rise to both a cardiomyopathy-like phenotype and prolonged QTc interval: either 1. creatine transporter deficiency gives rise to cardiomyocyte dysfunction that leads to a dilated cardiomyopathy phenotype. This pathologic response subsequently gives rise to "ion channel remodeling," commonly involving decreased outward potassium current, resulting in QTc prolongation or 2. creatine transporter deficiency directly results in potassium channel remodeling (including QTc prolongation that then cause cardiomyocyte dysfunction and subsequent cardiomyopathy development. Cardiomyopathy model mechanisms have involved both[28–30]. Diminished outward potassium current, particularly, transient outward potassium current, is commonly seen in cardiac hypertrophy and heart failure, and is likely contributing to abnormalities seen in both this animal model and our subjects[29,31].

Diminished potassium current or increased inward calcium current can further result in action potential duration (APD) prolongation which is reflected in a prolonged QTc[29]. Future animal model studies will be performed to directly measure potassium and calcium currents as a means of both determining mechanisms underlying QTc prolongation seen in this model for CTD therapy development. Additional studies can also be performed to determine whether ion channel remodeling precedes hypertrophy or vice versa.

Discrepant phenotypes between creatine synthesis knock-out vs creatine transport knock-out mice

One might predict that creatine synthesis enzyme inactivation would result in a similar phenotype to that seen in *Slc6a8*$^{-/y}$ because both scenarios lead to cardiac creatine depletion. This appears not to be the case for either human or mouse creatine system abnormalities[32]. Mice with guanidinoacetate methyltransferase (GAMT) null mutations appear to have less significant cardiac phenotype[33–35] than mice with creatine transport abnormalities. Creatine kinase inactivation also seems to confer a more significant cardiac phenotype when compared to *Gamt*$^{-/-}$ null mice [32,36]. Creatine is synthesized in the liver, pancreas, and kidney by arginine-glycine amidinotransferase (AGAT) and GAMT[5]. Mutations in each of these genes have been described and all result in intellectual disability and speech delay[5]. A survey of OMIM entries and review of literature suggests that patients with AGAT and GAMT mutations apparently have no cardiac disease associated with either defect. Mouse models of AGAT and GAMT have been evaluated for cardiovascular disease, however. One group demonstrated that germline *Gamt* deletion in mice yielded no significant cardiac phenotype, defined by no change in exercise tolerance and no difference in response to myocardial infarction (MI) compared to control. This was shown using limited echocardiographic and invasive hemodynamic datasets pre- and post MI[37]. Prior studies used cardiac MRI which is considered superior for cardiomyopathy diagnosis clinically[38], but leaves us unable to make direct comparisons between models. In the *Gamt*$^{-/-}$ mouse, baseline systolic and diastolic function appeared normal, but response to ischemia/reperfusion (I/R) injury showed ischemic contracture in two of four mutant mice, but no diminished cardiac systolic or diastolic function in controls[38]. While there seems to be divergent exercise capacity between *Gamt*$^{-/-}$ mice and *Slc6a8*$^{-/y}$ mice, *Gamt*$^{-/-}$ mouse response to I/R injury implies a significant cardiac phenotype. Importantly, a year-long *Gamt*$^{-/-}$ mouse cardiac MRI study differs from ours in that there appears to be significantly increased mortality in our cohort compared to controls over that time, while no such increased death was seen in their *Gamt*$^{-/-}$ cohorts[33].

Agat$^{-/-}$ mice showed similarities to both *Gamt*$^{-/-}$ mice as well as *Slc6a8*$^{-/y}$ mice. Like *Slc6a8*$^{-/y}$ mice, *Agat*$^{-/-}$ mice were significantly smaller than control mice (~13g vs 28g)[39]. Baseline imaging studies with cardiac MRI presumably showed no obvious differences in chamber dimensions between cohorts but comparable echocardiographic measurements are not available. *Agat*$^{-/-}$ mice did show both diminished systolic pressure and elevated end-diastolic pressure, suggesting impaired diastolic and systolic function[39].

While it is difficult to reconcile the cardiac phenotypic differences between creatine transport deficiency and creatine synthesis deficiencies, it is important to point out that

others have seen similar results to what we have found. Specifically, several groups demonstrated that contractile reserve is compromised concordant with depletion of creatine[6,40]. Neubauer et al. postulate diminished creatine transporter concentration and diminished creatine concentration in the failing heart by an undetermined mechanism[6]. This data may suggest that the creatine transporter serves additional regulatory functions in the heart beyond creatine transport. Whether such additional function of the creatine transporter exists and whether it could explain phenotypic differences between creatine transporter knock-out and creatine synthesis enzyme knock-out needs further investigation.

Conclusions and clinical recommendations

In summary, our findings suggest CTD results in ion channel remodeling and structural chamber remodeling that have been shown in other disease processes to ultimately result in increased arrhythmogenesis and increased sudden death risk. Mouse model experiments demonstrate similar findings and offer the possibility that future work may elucidate cardiac disease mechanisms. This work further suggests the need for a larger prospective multicenter study to aggregate subjects in order to better detail the breadth and depth of disease pathology seen in CTD patients. While such data is being collected, we recommend the following clinical precautions in managing CTD patients:

Clinical recommendations

1. We recommend all patients with a new diagnosis of CTD have an ECG to assess QTc length and for the presence of inferior T-wave abnormalities. Additionally, routine ECG evaluations at regular intervals are further recommended including before and after adding any chronic medication that is known or suspected of QTc prolongation.
2. When possible, avoid QT prolonging medications, including antiepileptic (Felbamate) or antiemetic drugs (ondansetron) that can act directly or indirectly on ion channels in both heart and brain.
    a. Avoid QT prolonging medications to minimize risk.
    b. The credible meds website (QTdrugs.org) is an excellent resource for this.
3. We recommend all subjects with a new diagnosis of CTD have a complete echocardiogram as well as subsequent echocardiograms on a routine basis to assess cardiac function and surveil for cardiomyopathy.
4. We recommend ambulatory ECG (Holter) monitoring if subject presents with concerning symptoms including palpitations, chest pain, pre-syncope and occasional routine monitoring to evaluate for occult arrhythmia.
5. Following episodes of hemodynamic compromise and/or paroxysmal change in awareness state, consider the need for cardiovascular work-up as a potential cause of the acute episode.

Supplementary Material

Refer to Web version on PubMed Central for supplementary material.

ACKNOWLEDGEMENTS

NCATS, NICHD, NIMH, and NHLBI intramural programs funded work. We express our sincere gratitude to the subjects and their families for supporting this work. We also thank the Association for Creatine Deficiencies. The *Slc6a8*$^{-/y}$ mice were provided by Dr. Laura Baroncelli (Italian National Research Council). We would like to acknowledge support by Lumos Pharmaceuticals and Ultragenyx. No author has financial relationships to disclose. We would also like to acknowledge the NHLBI pathology and mouse phenotyping cores for their assistance in data collection and data analysis.

REFERENCES

1. Rosenberg EH, Martinez Munoz C, Betsalel OT, et al. Functional characterization of missense variants in the creatine transporter gene (SLC6A8): Improved diagnostic application.Hum Mutat2007;28(9):890–896. [PubMed: 17465020]
2. Mercimek-Mahmutoglu S, Salomons GS. Creatine deficiency syndromes. In: Adam MP, Ardinger HH, Pagon RA, et al., editors. Genereviews((R)) Seattle (WA)1993.
3. Rosenberg EH, Almeida LS, Kleefstra T, et al. High prevalence of SLC6A8 deficiency in x-linked mental retardation.Am J Hum Genet2004;75(1):97–105. [PubMed: 15154114]
4. Newmeyer A, Cecil KM, Schapiro M, Clark JF, Degrauw TJ. Incidence of brain creatine transporter deficiency in males with developmental delay referred for brain magnetic resonance imaging.J Dev Behav Pediatr2005;26(4):276–282. [PubMed: 16100500]
5. Stromberger C, Bodamer OA, Stöckler-Ipsiroglu S. Clinical characteristics and diagnostic clues in inborn errors of creatine metabolism.J Inherit Metab Dis2003;26(2–3):299–308. [PubMed: 12889668]
6. Neubauer S, Remkes H, Spindler M, et al. Downregulation of the Na^+-creatine cotransporter in failing human myocardium and in experimental heart failure.Circulation1999;100(18):1847–1850. [PubMed: 10545427]
7. Guimbal C, Kilimann MW. A Na^+-dependent creatine transporter in rabbit brain, muscle, heart, and kidney. cDNA cloning and functional expression.J Biological Chem1993;268(12):8418–8421.
8. Salomons GS, van Dooren SJ, Verhoeven NM, et al. X-linked creatine-transporter gene (SLC6A8) defect: A new creatine-deficiency syndrome.Am J Hum Genet2001;68(6):1497–1500. [PubMed: 11326334]
9. van de Kamp JM, Betsalel OT, Mercimek-Mahmutoglu S, et al. Phenotype and genotype in 101 males with X-linked creatine transporter deficiency.J Med Genet2013;50(7):463. [PubMed: 23644449]
10. Anselm IA, Coulter DL, Darras BT. Cardiac manifestations in a child with a novel mutation in creatine transporter gene SLC6A8.Neurology2008;70(18):1642–1644. [PubMed: 18443316]
11. Nozaki F, Kumada T, Shibata M, Fujii T, Wada T, Osaka H. A family with creatine transporter deficiency diagnosed with urinary creatine/creatinine ratio and the family history: The third japanese familial case.Hattatsu Brain Dev2015;47(1):49–52.
12. Priori SG, Schwartz PJ, Napolitano C, et al. Risk stratification in the Long-QT syndrome.New England Journal of Medicine2003;348(19):1866–1874.
13. Baroncelli L, Alessandrì MG, Tola J, et al. A novel mouse model of creatine transporter deficiency.F1000research2014;3:228. [PubMed: 25485098]
14. Baroncelli L, Molinaro A, Cacciante F, et al. A mouse model for creatine transporter deficiency reveals early onset cognitive impairment and neuropathology associated with brain aging.Human Molecular Genetics2017;25(19):4186–4200.
15. McKeon A, Vaughan C, Delanty N. Seizure versus syncope.Lancet Neurology2006;5(2):171–180. [PubMed: 16426993]

16. Medford BA, Bos JM, Ackerman MJ. Epilepsy misdiagnosed as Long QT syndrome: It can go both ways.Congenit Heart Dis2014;9(4):E135–E139. [PubMed: 23750755]
17. Taggart NW, Haglund MC, Tester DJ, Ackerman MJ. Diagnostic miscues in congenital Long-QT syndrome.Circulation2007;115(20):2613–2620. [PubMed: 17502575]
18. Lang RM, Badano LP, Mor-Avi V, et al. Recommendations for cardiac chamber quantification by echocardiography in adults: An update from the American Society of Echocardiography and the European Association of Cardiovascular Imaging.J Am Soc Echocardiog2015;28(1):1–39.e14.
19. Levin MD, Lu MM, Petrenko NB, et al. Melanocyte-like cells in the heart and pulmonary veins contribute to atrial arrhythmia triggers.The Journal of clinical investigation2009;119(11):3420–3436. [PubMed: 19855129]
20. Yang ZH, Pryor M, Noguchi A, et al. Dietary palmitoleic acid attenuates atherosclerosis progression and hyperlipidemia in low-density lipoprotein receptor-deficient mice.Mol Nutr Food Res2019;63(12):1900120.
21. Kleiber M. The fire of life; an introduction to animal energeticsNew York: Wiley; 1961.
22. Meister J, BoneId DBJ, Godlewski G, et al. Metabolic effects of skeletal muscle-specific deletion of beta-arrestin-1 and −2 in mice.Plos Genetics2019;15(10):1–17.
23. Team RC. R: A language and environment for statistical computing2018.
24. Wickham H. Ggplot2, elegant graphics for data analysis2009.
25. Crilley JG, Boehm EA, Blair E, et al. Hypertrophic cardiomyopathy due to sarcomeric gene mutations is characterized by impaired energy metabolism irrespective of the degree of hypertrophy.Journal of the American College of Cardiology2003;41(10):1776. [PubMed: 12767664]
26. Ormerod JOM, Frenneaux MP, Sherrid MV. Myocardial energy depletion and dynamic systolic dysfunction in hypertrophic cardiomyopathy.Nature Reviews Cardiology2016;13(11):677–687. [PubMed: 27411403]
27. Maron BJ, Gottdiener JS, Bonow RO, Epstein SE. Hypertrophic cardiomyopathy with unusual locations of left ventricular hypertrophy undetectable by m-mode echocardiography. Identification by wide-angle two-dimensional echocardiography.Circulation1981;63(2):409–418. [PubMed: 6450004]
28. Cutler MJ, Jeyaraj D, Rosenbaum DS. Cardiac electrical remodeling in health and disease.Trends Pharmacol Sci2011;32(3):174–180. [PubMed: 21316769]
29. Hill JA. Electrical remodeling in cardiac hypertrophy.Trends Cardiovas Med2003;13(8):316–322.
30. Hill JA. Hypertrophic reprogramming of the left ventricle: Translation to the ECG.J Electrocardiol2012;45(6):624–629. [PubMed: 22999493]
31. Wang Y, Hill JA. Electrophysiological remodeling in heart failure.Journal of Molecular and Cellular Cardiology2010;48(4):619–632. [PubMed: 20096285]
32. Heinrich T, IJ S. Creatine—a dispensable metabolite?Circ Res2013;112(6):878–880. [PubMed: 23493302]
33. Schneider JE, Stork L-A, Bell JT, et al. Cardiac structure and function during ageing in energetically compromised guanidinoacetate n-methyltransferase (GAMT)-knockout mice – a one year longitudinal mri study.J Cardiov Magn Reson2008;10(1):9.
34. Schneider JE, Tyler DJ, ten Hove M, et al. In vivo cardiac 1h-mrs in the mouse.Magnetic Resonance in Medicine2004;52(5):1029–1035. [PubMed: 15508174]
35. Mt Hove, Makinen K, Sebag-Montefiore L, et al. Creatine uptake in mouse hearts with genetically altered creatine levels.Journal of Molecular and Cellular Cardiology2008;45(3):453–459. [PubMed: 18602925]
36. Dzeja PP, Hoyer K, Tian R, et al. Rearrangement of energetic and substrate utilization networks compensate for chronic myocardial creatine kinase deficiency.The Journal of Physiology2011;589(21):5193–5211. [PubMed: 21878522]
37. Craig L, Dunja A, Dana D, et al. Living without creatine: Unchanged exercise capacity and response to chronic myocardial infarction in creatine-deficient mice.Circ Res2013;112(6):945–955. [PubMed: 23325497]

38. Mt Hove, Lygate CA, Fischer A, et al. Reduced inotropic reserve and increased susceptibility to cardiac ischemia/reperfusion injury in phosphocreatine-deficient guanidinoacetate-n-methyltransferase–knockout mice.Circulation2005;111(19):2477–2485. [PubMed: 15883212]

39. Faller KME, Atzler D, McAndrew DJ, et al. Impaired cardiac contractile function in arginine: Glycine amidinotransferase knockout mice devoid of creatine is rescued by homoarginine but not creatine.Cardiovascular Research2018;114(3):417–430. [PubMed: 29236952]

40. Tian R, Ingwall JS. Energetic basis for reduced contractile reserve in isolated rat hearts.Am J Physiol-heart C1996;270(4):H1207–H1216.

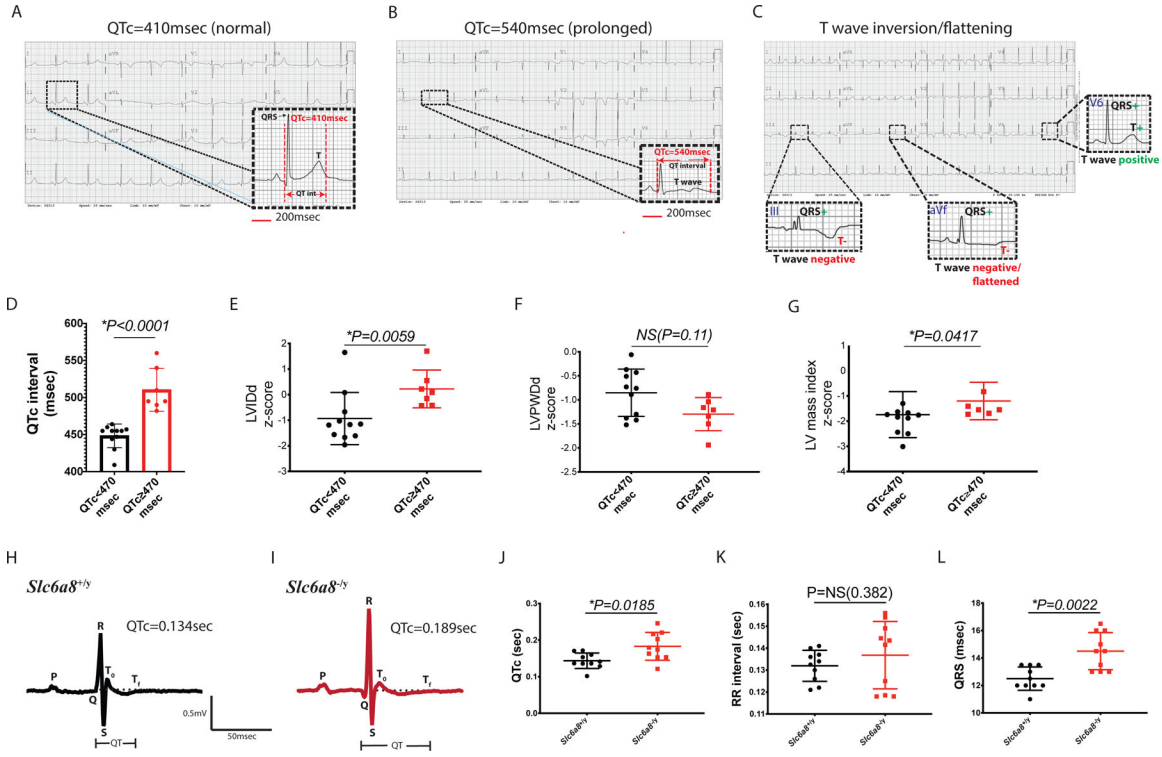

Figure 1. Human and mouse ECGs demonstrate prolonged QTc and echocardiographic data consistent with cardiomyopathy.

Human ECG from CTD subjects showing (A) normal QTc, 410msec, inset scale bar=200msec (B) prolonged QTc, 540msec, inset scale bar=200msec and (C) normal QTc, but T-wave inversion and flattening. Inset "v6" demonstrates upward going QRS tracing (+) as well as upgoing T-wave(+) (normal relationship), while "III" shows upward going QRS(+) and *downward* going T-wave(−) (inverted) indicating T-wave abnormal QRS:T-wave relationship. Lead "aVf" shows "flattened" T-wave. (D)Scatter plot shows QTc distributions from QTc<470msec and QTc≥470msec cohorts. Scatterplots show echocardiographic parameters for CTD subject by QTc cohort for (E) LVIDd z-score (F)LVPWDd z-score and (G) LV mass index z-score. Representative mouse ECG tracings of control (H) *Slc6a8*$^{+/y}$ and (I) *Slc68a*$^{-/-y}$ mice showing prolonged QT in latter. Scale bars = 0.5millivolts and 50milliseconds. T_0 represents T-wave onset, while T_f denotes T-wave termination. Scatter plots showing mean±SD per cohort of (J) corrected QT interval (QTc) and (K) RR interval (L) QRS interval. Mann-Whitney test used to test for significance. Abbreviations: CTD, creatine transporter deficiency; ECG, electrocardiogram; QTc, corrected QT interval (in milliseconds). LV, left ventricular; LVIDd, LV internal dimension(diastole); LVPWDd, LV posterior wall dimension(diastole). Note: each ECG recorded using standard sweep speed=1mm grid=0.04seconds.

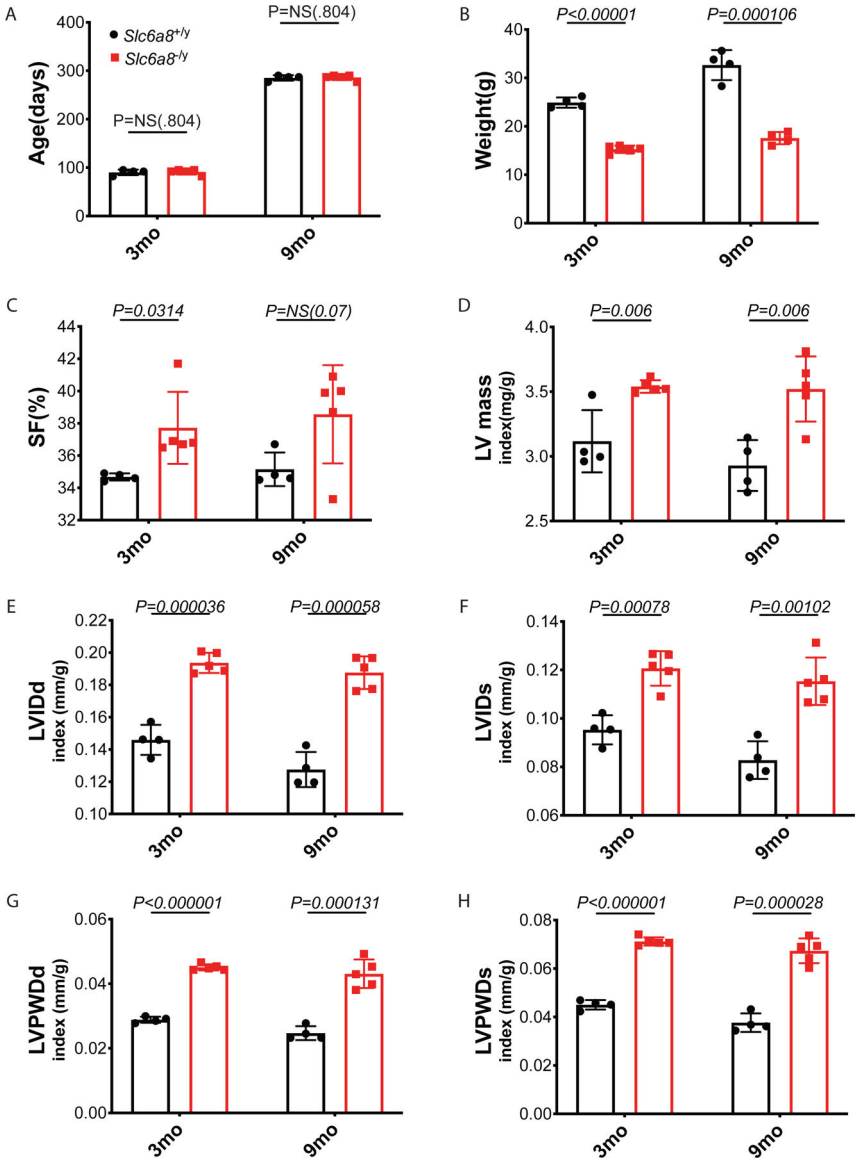

Figure 2. *Slc68a*$^{-/y}$ mouse model echocardiographic data 3 and 9 months demonstrates preserved systolic function, LV chamber dilation, and increased LV was thickness.

Scatter plots demonstrate echocardiographic demographic data including: (a) age (b) weight as well as systolic function (c) FS(%) and chamber structural parameters (d) LV mass index (e) LVIDd (f) LVIDs (g) LVPWDd and (h) LVPWDs in both *Slc68a*$^{-/y}$ mice and controls. Imaging was performed under light sedation. Data are presented as mean±SD, and significance was assessed using Mann-Whitney test. Abbreviations: FS, fractional shortening; LV left ventricular; LVIDd, LV internal dimension(diastole); LVIDs, LV internal dimension(end-systole); LVPWDd, LV posterior wall dimension(diastole); LVPWDs, LV posterior wall dimension(systole).

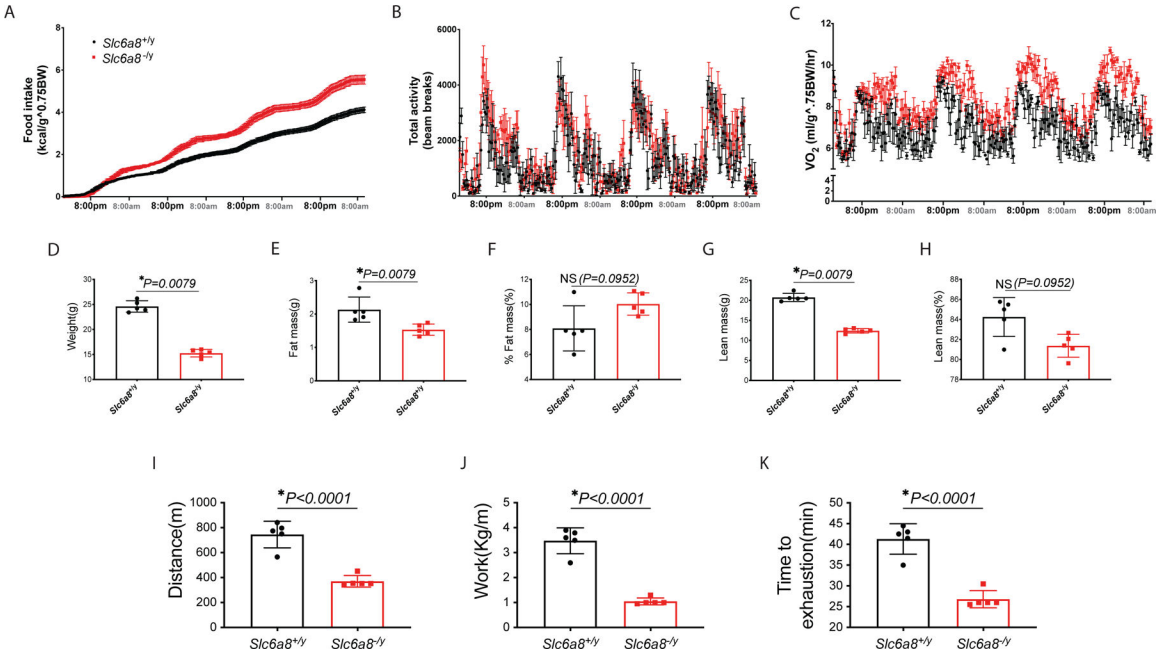

Figure 3. 3-month *Slc6a8*$^{-/y}$ mice show increased VO_2, diminished exercise capacity and shorter time to exhaustion.

Indirect calorimetry was performed using Oxymax CLAMS system. *Slc6a8*$^{-/y}$ mice show increased normalized food intake (A) and oxygen consumption (VO_2)(C) despite mean activity(B) being roughly equivalent. Body composition determined by EchoMRI demonstrate decreased (D) weight (E) fat mass (G) lean mass and (H) %lean mass in *Slc6a8*$^{-/y}$, while %fat mass (F) appeared greater in *Slc6a8*$^{-/y}$ mice. **Exercise testing** shows *Slc6a8*$^{-/y}$ mice have diminished (I) distance traveled and (J) work expended during exercise. This correlates with much shorter (K) time to exhaustion during excise. Data are displayed as mean±SD, and significance was assessed using Mann-Whitney test.

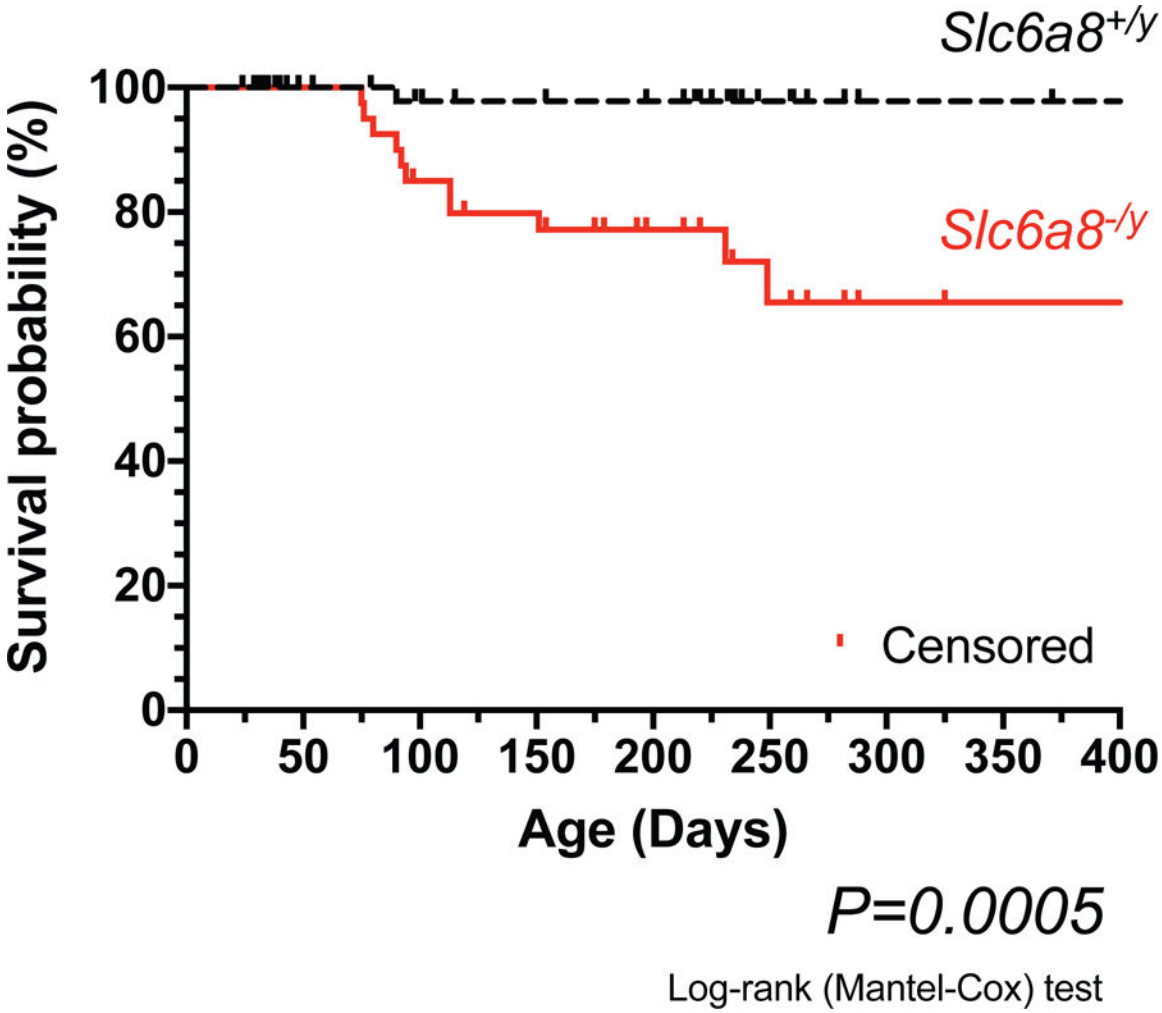

Figure 4. *Slc6a8*$^{-/y}$ mice show significantly diminished survival probability and increased unexpected death incidence when compared to controls.

(Log-rank (Mantel-Cox) test, *P=0.00050*).

Table 1.

Creatine transport deficiency subject ECG and Echocardiographic summary findings

	QTc<470msec	QTc≥470msec	*P-value*
# of subjects	11	7	NS
Age (years)	8.0±4.4	6.5±2.8	NS
Wt (kg)	22.6±9.9	17.3±7.7	NS
BSA	0.85±.27	0.72±.21	NS
Electrocardiogram findings			
Heart rate (bpm)	97.5±23.3	95.9±12.5	NS
Rhythm	All NSR	All NSR	NS
P axis (degrees)	42.3±19.1	38.3±25.0	NS
QRS axis (degrees)	76.0±19.9	56.0±37.4	NS
T axis (degrees)	**38.6±21.0**	**16.4±15.7**	***P=0.047***
PR interval (msec)	121.7±17.2	129.1±14.4	NS
QRS interval (msec)	79.6±6.3	79.7±9.4	NS
QT interval (msec)	**357.8±38.3**	**405.3±43.4**	***P=0.047***
QTc interval (msec)	**448.3±15.9**	**510.3±29.0**	***P<0.0001***
T wave abnormality	**3/11**	**6/7**	***P=0.049***
Echocardiographic findings			
EF(%)	64.2±2.1	65.7±3.5	NS
FS(%)	37.8±2.4	39.7±5.0	NS
LVIDd(mm)	33.9±5.2	34.7±4.1	NS
LVIDd z-score	**−0.93±1.0**	**0.22±0.74**	***P=0.0059***
LViDs(mm)	20.0±6.7	21.1±3.2	NS
LViDs z-score	−0.86±.75	−0.32±1.27	NS
IVS (mm)	5.6±0.9	5.1±0.7	NS
IVS z-score	−1.2±0.5	−1.3±0.6	NS
LVPWDd(mm)	**5.7±0.8**	**5.0±0.6**	***P=0.0183***
LVPWDd z-score	−0.85±.49	−1.30±.35	NS(.11)
LV mass (g)	47.0±17.5	42.8±14.9	NS
LV mass z-score	−1.5±0.9	−0.95±.76	NS(.065)
LV mass indexed	54.2±10.1	57.6±9.5	NS
LV mass index z-score	**−1.7±0.9**	**−1.2±0.7**	***P=0.0417***
Pro-BNP (pg/mL) (# of pts with samples)	147±98.0(5)	270±102(3)	NS

Abbreviations: AV, atrioventricular; BSA, body surface area; EF, Ejection fraction; FS, Fractional shortening; ECG, electrocardiogram; HR, heart rate; bpm, beats per minute; LVIDd, left ventricular dimension in diastole (2-dimenstional); LVIDd z-score, LVIDd normalized to individual subject's BSA; LVIDs, left ventricular dimension in systole (2-dimenstional)); LVIDs z-score, LVIDs normalized to individual subject's BSA LVPWDd, left ventricular posterior wall dimension (thickness) in diastole; LVPWDd z-score, LVPWDd normalized to individual subject's BSA; LV, left ventricular; mm, millimeters, measurement units; NSR, normal sinus rhythm; QTc, corrected QT interval (using Bazett's formula, where QTc=QT/√RR); NS, not significant; pts, subjects; pro-BNP, pro-brain natriuretic peptide; pg/mL, picogram per milliliter; All above statistics were performed using non-parametric T-test(Mann-Whitney).